DISORDERED SYSTEMS AND MATERIALS SCIENCE

The Laboratoire Léon Brillouin is progressively putting in place a pole of research in the field of materials science, in strong relationship with external laboratories. Indeed, it is the role of a national research infrastructure such as LLB to train the scientists working in french applied research and industrial laboratories, and to give them access to its characterization facilities.

The research at LLB in materials science covers two main domains : soft matter and metallurgy (in the broad sense, i.e. including ceramics, metal matrix composites, etc...). The results concerning soft matter are included in the chapter "Chemical Physics and Biology" of this report.
In the domain of metallurgy and ceramics, the properties of technological interest depend on the defect properties and on the defect structure of the material at the atomic (vacancies, impurities,...) or at the mesoscopic (dislocations, porosities,...) level. This is why materials science requires a fundamental corpus of knowledge on defects and disorder. In particular, the fundamental study of atomically disordered systems allows to develop theoretical models, and to validate numerical simulations (Monte-Carlo, molecular dynamics, etc...) which are then applied to understand "real" materials. Particularly important is the extrapolation of their properties at long time in operating conditions, and the prediction of their behaviour under thermal or irradiation-induced ageing.
At the interface between the study of disordered systems and materials science is physical metallurgy, working on model systems (e.g. phase transformations in binary alloys, etc...).

1. DISORDERED SYSTEMS

1.1. Introduction

The scientific activity of LLB in the field of disordered systems is mainly concentrated on the study of local atomic arrangements in topologically or chemically disordered solids or liquids, by elastic diffuse neutron scattering. Two instruments are entirely devoted to these studies :

- the 7C2 diffractometer, installed on the "hot" source, with short wavelength (generally ˜ 0.7 Å) neutrons, and equipped with a 640 cell position sensitive linear multidetector, for liquid and amorphous systems;
- the G4.4 diffractometer, installed on a "cold" neutron guide, managed by ONERA and CEA/LSI, with time-of-flight analysis, devoted to the "in situ" high temperature study of local order in single crystals.

In the case of systems presenting a tendency towards phase separation, complementary studies by Small-Angle Neutron Scattering (SANS) are necessary.
Some studies of dynamics, mainly on glass transition, are also performed at LLB by external users, in particular with the time-of-flight inelastic spectrometer MIBEMOL.

1.2. Metallic alloys : local order, kinetics

This thematics is mainly developed at LLB by the team of LEM (ONERA-CNRS, R. Caudron et al).
A systematic "in situ" high temperature study of elastic diffuse neutron scattering in a series of f.c.c. binary transition metal alloys, performed on G4.4, has allowed a detailed understanding of their chemical order-disorder properties, and a fruitful dialogue with the statistical physics theory of alloys. This 10-years programme was concluded in 1997 by the PhD thesis of D. Le Bolloch on $Pt_{1-x}V_x$ alloys. In the frame of this work, it was in particular shown that, although $Pt_{0.75}V_{0.25}$ long-range orders below T_c = 500°C with superstructure diffraction peaks at (1 1/2 0), the maxima of the diffuse intensity above T_c are at the (100) positions. Moreover, the diffuse intensity for another concentration, x=1/9, displays a splitting around (100) with maxima at incommensurate positions. It was found that, despite this strong concentration dependence of the diffuse intensity shape, the Effective Pair Interactions deduced of the experimental data by a reverse Monte-Carlo method, are nearly concentration independent, in contradiction with *ab initio* theories. A high temperature expansion of the mean-field theory was developed, and explained successfully the origin of this splitting, and its dependence with concentration and temperature.

This work is now being extended to kinetic phenomena (PhD thesis of X. Flament). Mean-field theory suggests for Pd_3V two different spinodal (instability) temperatures for the two ordering wave-vectors, e.g. (100) and (1 1/2 0). Monte-Carlo simulations and preliminary synchrotron X-ray experiments are in agreement with these predictions.
Several studies of local order and concentration fluctuations in various crystalline (Ni_2Cr, Ni-based superalloys) or amorphous (Fe_2Zr, $Ti_{84}Si_{16}$, selenite glasses) systems have also been performed by other groups (LSI/Palaiseau, CEMES/Toulouse, LLB, MPI/Stuttgart, Bulgarian Academy of Sciences (Sofia)).

1.3. Local order in quasi-crystals and their liquid precursors

If the indexation of diffraction peaks in quasi-crystals can be made with success, the problem of positions of specific types of atoms is far from being resolved. Is there or not chemical disorder ? This has an important impact on our understanding of the origin of the stability of these materials at room temperature : i.e. are they stabilized by defects when cooling from high temperature ? If such a disorder exists, it should manifest itself by an elastic diffuse scattering in the neutron or X-ray diffraction spectra. Scarce information existing up to now led to conflicting results. The advantage of neutrons over X-rays is the easiness to obtain absolute cross-sections and the possibility to separate experimentally the inelastic thermal diffuse scattering due to phonons. The difficulty with neutrons is their sensitivity to hydrogen contamination, and the lower q-resolution to well separate the Bragg peaks. We have therefore undertaken a study at LLB on this subject (PhD thesis of N. Schramchenko) in collaboration with LEM (ONERA-CNRS) and CECM-Vitry, where the samples are made.
First experiments performed on G4.4 at LLB on a single grain of Al-Pd-Mn, allowed to observe at room temperature a diffuse scattering far from the Bragg peaks. Normalized, it is in agreement with the theoretical disorder term from an approximant phase ξ' of similar composition. The data treatment is delicate, because one has to correct for a very large number of very small Bragg peaks.

The preliminary work presented in the previous LLB report (1995-96) on liquid precursors of Al-Pd-Mn, has been extended and completed in the frame of a multi-laboratory collaboration (LPS-Orsay, LTPCM-Grenoble, LLB-Saclay, PhD thesis of V. Simonet, Orsay, 1998, see highlight). The set of diffuse neutron scattering measurements performed at LLB on 7C2, and subsequently extended at ILL on D4B, confirmed the presence of a local order reminiscent from the solid, and could be fitted by a cluster-based ($Al_{12}Mn$ icosahedron) numerical simulation.
Polarized neutron scattering experiments performed at D7, ILL, have confirmed the appearance of a magnetic signal in the liquid state, deduced previously from coupled 7C2 neutron scattering and magnetic susceptibility measurements.

1.4. II-VI and IV-VI liquid compounds

The classical semi-conductors of group IV (Si, Ge) as well as the III-V compounds (GaAs, GaSb) undergo at the melting point a semi-conductor $\rightarrow$ metal transition, associated to a change of coordination number ($4 \rightarrow 6$). On the contrary, some II-VI compounds (CdTe, ZnTe) remain semi-conducting and tetrahedrically coordinated in the liquid state. To understand the origin of this behaviour, we have undertaken, in collaboration with the University of Liège, an experimental and theoretical study of Cd_xTe_{1-x} in all the concentration range (PhD thesis of G. Prigent).
Monte-Carlo simulations in the frame of a tight binding model, have shown that the local order in these systems is mainly governed by the competition between the $s \rightarrow p$ promotion and the gain in binding energy (resonance between sp^3 orbitals). The charge transfer plays only a small role. CdTe remains semi-conductor, because the s level of Cd and the p level of Te are close in energy.
A double metal $\leftrightarrow$ semi-conductor $\leftrightarrow$ metal transition versus composition in the liquid state was observed experimentally from electrical measurements performed at the University of Metz. A fine analysis of neutron scattering (obtained on 7C2) and EXAFS data suggests a coexistence of metal Cd-rich and semi-conducting CdTe-rich domains of nanometric size for $x > 0.5$.

On the same subject, the team of University de Liège observed on 7C2 an astonishing re-entrant Peierls distortion in several IV-VI compounds : SnS, SnSe, GeSe and GeTe (PhD thesis of D. Raty) : the Peierls distortion, observed at low temperature and which disappears when heating in the crystalline state, is recovered in the liquid state.

1.5. Fundamental structural studies of simple fluids

Very precise Small-Angle Neutron Scattering experiments, performed on noble gas (e.g. krypton) by an italian group of the University of Firenze (R. Magli et al.), succeeded to show, for the first time, the role of irreducible three-body forces in the interatomic potential. Density fluctuations in these fluids have been measured in function of temperature and pressure and near the critical point.

1.6. Critical and supercritical fluids

Water is always an important and "hot" topic and gave rise to many studies where the structure and H-bond dynamics have been explored in various states, including metastable states under pressure and water in confined geometries (see the chapter "Chemical Physics and Biology" of this report). In particular, recent modelisation of LLB neutron diffraction experiments suggest strongly that two forms of liquid water may coexist at very low temperatures, possibly shedding light on why water has such unusual properties compared to other liquids. These structural and dynamic studies have been extended to water in supercritical state.

Supercritical water presents physical and chemical properties, e.g. viscosity and dielectric constant, which differ greatly from those of the liquid water. In particular, it is possible to dissolve in supercritical water organic or mineral substances, which are hardly soluble in normal liquid water. This is of great interest, in particular for depollution applications.
In view of developing these techniques, a "Club of Supercritical Fluids applied to Nuclear Industry" has been created in 1994. M.C. Bellissent-Funel chairs this group since 1998. It was decided to study at LLB by neutron scattering the local structure and dynamics of critical and supercritical fluids (water, CO_2, aqueous solutions), in order to validate Molecular Dynamics simulations (LPTL, University of Paris VI).

The partial pair correlation functions $g_{OD}(r)$, $g_{DD}(r)$ and $g_{OO}(r)$ in supercritical heavy water (T=380°C, pressure : 600 bar, density : 0.73 g/cm^3) were determined by a reverse Monte-Carlo method from the 7C2 neutron data obtained on D_2O and two isotopic H_2O/D_2O mixtures, and from X-ray data (which gives the O-O partial structure factor). The structure of supercritical water is very different from that of water in ambient conditions. Nevertheless, modelisation of these data by Molecular Dynamics simulations show clearly that in dense supercritical water, although the tetrahedral arrangement of water molecules is lost, some hydrogen bonding is still present, contrary to previous statements of other authors.
SANS study of supercritical heavy water showed a large increase at small q (0.07 to 0.36 Å^{-1}) due to the divergence of density fluctuations at the critical point, and allowed the first measurement of the critical correlation length ξ_0 for water; the value, 1.36 ± 0.06 Å, is in fair agreement with theoretical predictions.
A first study of the (picosecond range) dynamics of supercritical H_2O by incoherent inelastic and quasielastic neutron scattering, performed by LLB researchers on IN6 at ILL, allowed to determine the evolution of D (translational diffusion coefficient of the water molecules), L (jump distance) and τ_0 (residence time) as a function of the density of the medium. D and L increase strongly as the density decreases. τ_0 is ten times shorter than that measured in liquid water at room temperature.

Simple fluids (CO_2, SO_2) or fluid mixtures (H_2O-benzene, CS_2-benzene, CS_2-C_6F_6, ...) are also the object of structural studies in the critical and supercritical states (LASIR, Lille, LPCM, Bordeaux, Universities of Lisboa and of Roma III).

1.7. Phase separation

Several studies performed by external laboratories approached the problem of phase separation in solids and liquids.

Isotope ordering of hydrogen and deuterium, predicted theoretically by Prigogine in 1954, was proved for the first time at LLB by an international team led by M. Bienfait (CRMC2, Marseille) (see highlight) : a clustering process of isotopic hydrogen mixtures H_2-D_2, adsorbed in order to form one monolayer on graphite (0001), was observed from 8 K downwards, at and above monolayer completion, by SANS and neutron diffraction measurements. This trend towards phase separation depends strongly on coverage and isotopic concentration.

A remarkable closed-loop miscibility gap has been found in the liquid tellurium-sulfur ($Te_{1-x}S_x$) binary diagram around x = 0.4, which is a unique observation in an inorganic system. Neutron diffraction measurements performed on 7C2, showed that this is directly related to a sudden change of the tellurium coordination at high temperature, from nearly 3 for $x < 0.4$ (as in pure Te), to around 2 for $x > 0.4$ (PhD thesis of M.V. Coulet, CTM Marseille).

A systematic study by neutron scattering of the local order of several liquid alloys (Mn-Sb, Mn-Ge, Ga-Pb), presenting a miscibility gap at lower temperature, has been undertaken on 7C2 by a team of the University of Metz (J.F. Gasser et al). It allowed to test interatomic potentials obtained by electronic structure calculations, and to explain the anomalous behaviour of electronic conductivity and thermal expansion in these alloys.

The understanding of the role of an uniaxial elastic strain on the phase separation in binary metallic alloys presenting a large size effect between the two atomic constituents, is object of a detailed small-angle neutron scattering work by the austrian team of University of Vienna associated to LLB (O. Blaschko†, M. Prem). In particular, they could show that such strain applied during thermal treatment induces an anisotropy in the shape of the precipitates formed in CuRh, which can be explained by a misfit compensation mechanism.

1.8. Dynamics. Glass Transition

The study of relaxation processes in liquids near the glass transition has been the object of several studies performed by C. Alba-Simionesco (CPMA, Orsay). Combination of quasi-elastic spectra obtained in a wide frequency range show the existence of two relaxation processes. Several studies were performed under pressure, in order to separate the respective roles of volume reduction due either to pressure increase or to temperature decrease in the structural arrest near the glass transition.
Several other studies of the dynamics of disordered systems were performed by external laboratories at the LLB, mostly on the time-of-flight inelastic instrument MIBEMOL. These include :
- the first study of the vibrational density of states of carbon nanotubes (University of Montpellier);
- measurement of the mobility of HD molecules adsorbed on incommensurate Kr plated graphite, which confirmed the existence of a reentrant fluid phase, squeezed in between the commensurate and incommensurate phases (collaboration between Universities of Mainz, Germany, and of Marseille, France);
- study of the vibrational dynamics in plastic crystals (where a periodic lattice coexists with translational disorder) (Universities of Augsburg and Munich, Germany);
- dynamical behaviour of molecules confined in the pores of SiO_2, which allowed to distinguish non-rotating molecules adsorbed on the pore walls, and rotating molecules within the pores (University of Kiel, Germany);
- influence of the cross-linking ratio on the dynamics of the glass transition (University of Montpellier).

1.9. Evolution and Perspectives

The specificity of neutron-matter interaction leads to develop its use on samples held in extreme conditions (e.g. high temperatures, high pressures,...), as exemplified by the LLB studies on supercritical fluids. In this aim, an important upgrade of the 7C2 diffractometer for liquids is planned, in collaboration with several external french laboratories. It consists in :

- developing high temperature devices, in particular contactless heating methods : gas levitation technique for insulating liquids, and electromagnetic levitation for conducting liquids;
- increasing the counting rate (new more efficient multidetectors, improved neutron optics), in particular to improve the signal-to-noise ratio in the case of the small samples required by the above techniques.

This instrument upgrade will allow new applications in several important fields :

- materials processing : local structure of the liquid formers of metallic or oxide materials prepared by solidification;
- geophysics : "in situ" study of the high density forms of silicate glasses.

2. MATERIALS SCIENCE

2.1. Introduction

Materials Science aims to understand the properties of solid systems in their full complexity, and to optimize these properties by acting on the composition, atomic structure, and microstructure. This is a different approach to that of condensed matter physics, which focuses on model systems to study a given property or phenomenon. Obviously, materials science has an immediate bearing on industry and applications.
Neutrons are an ideal probe for studying the structure of materials, particularly because of their low absorption, which makes it possible to work on centimetre-thick parts, and the relative ease with which experiments can be carried out under complex or extreme conditions, such as high temperatures or applied stress.

Research currently under way at LLB includes studies in :

- Residual stress evaluation in complex systems,
- Evolution of textures with thermal or mechanical processing,
- Structure heterogeneity, precipitation, ageing of materials,
- Properties of coated glasses and gratings.

Studies on industrial materials are usefully complemented by studies of model materials that are easier to interprete. Methods for analysing the reciprocal lattice (neutron and X-ray scattering) and the real lattice (electron microscopy, atomic probe, near-field microscopy) are complementary, and always used together, especially for complex industrial materials.

2.2. Residual stresses

In the last decade, the use of neutron diffraction for stress analysis in components of technological interest has strongly developed. In fact, the unique properties of neutrons, in particular their high penetration depth, mean that neutron diffraction is the only non-destructive technique which enables the stress field evaluation within a defined volume in a bulk sample. Diffraction of hard X-rays, such as those available at the ESRF (Grenoble), open new possibilities, but also present technical difficulties and limitations (e.g. shape of the gauge volume).
In the last years, a new diffractometer entirely dedicated to stress analysis, DIANE (G5.2), was built up at the LLB in Saclay, in collaboration with the italian INFM (Istituto Nazionale di Fisica della Materia). It has been designed in order to meet engineering requirements : good spatial resolution (of the order of 1 mm^3), accurate positioning of the specimen in three orthogonal directions, an adequate space for manipulation of heavy and cumbersome samples on the diffractometer, good instrumental resolution (high monochromator take-off angle), and fast data collection (Position Sensitive Detector).
A widely spread activity has been developed in the last two years at the LLB in the field of residual stress analysis, partly in collaboration with the University of Reims-Champagne-Ardenne (Prof. A. Lodini).

The main fundamental studies performed at the LLB in the field of residual stress analysis are summarized below :

Microstrain evaluation. Measurements of the diffraction line profile on DIANE at LLB allowed for the first time to characterize non-destructively the plastic region (i.e. its size and the maximum strain) at the tip of a crack in a stainless steel fatigue test specimen (PhD thesis of K. Hirschi, see highlight).

Residual stresses in metal matrix composites (MMC). We have studied and modelized the effect of plasticity on the thermally induced residual stresses in an Al matrix MMC reinforced with SiC particles (PhD thesis of R. Levy-Tubiana, in collaboration with M. Fitzpatrick, The Open University, U.K., and A. Baczmanski, University of Krakow, Poland).

Strains in geological materials. Elastic residual strains, required by the natural continuity of solids, originate in the rocks during the fold of the upper crust. Neutron diffraction is the only technique which allows to determine the internal strain tensor in polycrystalline rocks. For the first time, residual elastic strains have been determined in polycrystalline samples of geological interest (quartzites). The components of the strain tensor, determined on DIANE at LLB, are weak in absolute value, but significant. These residual elastic strains were found to disappear in recristallized samples. An hydrostatic compressive state was also found in one sample, and is probably due to the presence of secondary phase inclusions (J.C. Guezou et al, University of Cergy-Pontoise).

Parallel to this fundamental activity, great effort is made to **open the neutron diffraction technique for stress analysis to industrial users**. To this end, we are involved in several international programs and industrial collaborations.

a) **VAMAS TWA 2O** is an international programme, the objective of which is to establish accurate and reliable procedures for making reproducible and standardized non-destructive neutron diffraction residual stress measurements. It includes representatives from industry, universities and 13 neutron sources, in Canada, Europe, Japan and the USA. Different types of samples, in which residual stresses have been introduced by various procedures, are examined by the participating neutron sources, according to a common protocol. In the last two years, an aluminium alloy shrink-fit and plug has been examined for "round robin" inter-laboratory comparison. The results obtained on DIANE allow to classify this instrument as one of the most performants.

b) **TRAINSS** is a 4-years (1998-2001) european network, of the Brite-Euram III programme, aimed to train european industrial laboratories to the use of neutron diffraction for determination of internal stresses. The TRAINSS network groups 4 neutron sources (among which LLB), 6 university laboratories (among which ENSAM, Paris), and 10 industrials which bring specific problems (among which SNCF and PSA-Peugeot-Citroen). Two weeks per year of neutron beam time are devoted to this programme on the DIANE diffractometer. SNCF is interested in the influence of residual stresses on the propagation of cracks in the wheel axles of railway engines and carriages. The PSA problem is the determination of residual stresses in the discs of motor-car brakes.

c) Two other contracts with french industry have been initiated recently : with SNECMA (residual stresses in a Ti matrix-SiC fiber MMC, for compressor discs and blades of airplane motors), and with Aerospatiale (residual stresses in a welding between aluminium alloy plates for Airbus).
EDF financed a PhD thesis, submitted in 1997 (E. Pluyette), which allowed to realize a numerical modelization of the DIANE diffractometer, aiming to improve the measurement of residual stresses across interfaces (e.g. a bimetallic welding).

d) Various studies of residual stresses in technological components were made by external laboratories, in particular :

- the stress profile was measured along the throat of automotive gears, which had undergone a surface treatment (R. Magli et al, University of Firenze and LLB);
- the stress gradient could be resolved in a ceramic (AlN) plate as thin as 0.6 mm, which is well below what is commonly achieved in neutron stress analysis, and proves the excellent performance of DIANE (L. Pintschovius, Kf Karlsruhe);
- residual strains and stresses in MMC's, weldings and brazings for nuclear fusion technology (NET / ITER programme), coated materials, etc... (University of Reims, University of Ancona, ENEA (Italy), The Open University (UK)).

2.3. Textures

Crystallographic texture (preferred orientation of grains) is one of the parameters describing the microstructure of a polycrystalline material, which controls partly its mechanical properties. In metallic alloys, the texture appears during the solidification, then transforms during rolling or wiredrawing, and ultimately during recrystallization. The understanding and the mastering of its texture during thermomechanical and/or annealing treatments are necessary in order to optimize the mechanical behaviour of a material.

Neutron diffraction is the best technique for obtaining precise texture of bulk specimens (~ 1 cm^3), under the form of a distribution function of crystalline orientations. Its use is in particular necessary in the case of coarse-grained materials (= a few mm^3), where conventional X-rays are inapplicable.

LLB has a diffractometer specially devoted to the determination of crystallographic textures : 6T1, equipped with an Euler craddle. The study of textures at LLB is made in strong collaboration with the Laboratoire de Métallurgie Structurale (LMS) of the Orsay University (T. Baudin, R. Penelle), where are performed complementary studies by EBSD (Electron BackScattered Diffraction) and numerical simulations of the evolution of the microstructure.

An important number of experiments was made to determine the texture in two-phase materials of technological interest, and to study the relation between texture components of each phase. Let us mention two of them :

- In the two-phase Ti-based high strength alloy ßCEZ, developed for use in the compressor of jet engines, it was found that the sharpness of the crystallographic texture (but not its components which follow the usual orientation relationship) is strongly dependent on the morphology of the α-phase. This has important implications on the optimization of the thermomechanical treatments (LLB and University of Orsay).
- In a welded joint of 316L stainless steel containing coarse grains of f.c.c. austenite and a very small content (5%) of b.c.c. δ ferrite, the neutron diffraction analysis showed that on a macroscopic scale, both phases are in a cube-cube relationship, with a fiber texture [010] along the solidification direction. This unusual result shows that solidification has been duplex itself, with a solidification front and the growth of both ferrite and austenite primary phases; it is introduced in the numerical codes predicting the mechanical behaviour of the welding (J.L. Béchade et al, SRMA, Saclay, and Ecole des Mines de Paris).

Furthermore, the recrystallization process has been more specially investigated in different materials :

- The texture of Ti-Al based intermetallic alloys, considered for aerospace industry, influences their ductility and creep behaviour. A study of the dependence of texture on forging and (dynamic and static) recrystallization conditions has been undertaken, in order to suppress or reduce this texture and optimize the mechanical properties of the material (PhD thesis of Y. Hersart, University of Orsay).
- In a $Fe_{0.5}Ni_{0.5}$ alloy, neutron diffraction, associated to Transmission Electron Microscopy and EBSD experiments, allowed to follow the growth kinetics of the cube texture (which is interesting for magnetic applications) to the detriment of the deformation ones, after cold rolling and annealing. This study allows to improve the simulations of the recrystallization (LLB and LMS).

Since several years, a part of the texture activity at LLB is dedicated to the study of geological materials. In particular, neutron diffraction coupled to microstructural observations allowed, in quartzites coming from the betic zone of Spain, to identify two main components, {1-210} <10-10> and {1-101} <1-120>, which have been associated respectively to the deformation and the recrystallization (University of Cergy-Pontoise).

2.4. Phase analysis

A research programme has been undertaken since 1997 at LLB by the Direction of Nuclear Reactors in CEA, Saclay, to characterize and study hydrogen-containing zircaloy-4 alloys, used as fuel cladding in Pressurized Water Nuclear Reactors (PWR) (see highlight). Because of its low thermal neutron absorption and incoherent cross-sections, Zr is a very favorable material for such studies. In a single experiment, it was possible to obtain the total

hydrogen content with high sensitivity and precision (< 20 ppm weight), the hydrogen content in hydride form, the crystallographic characterization of precipitates (hydrides and Laves phases), and to follow "in situ" up to 500 °C the influence of H on the thermal expansion of zircaloy-4 and the thermal dissolution of hydrides. This last information allowed to determine the solubility of H in the material between room temperature and 500 °C.

2.5. Nanopowders and sintering

The last two years have seen an important development of studies in this domain by neutron scattering (SANS and diffraction). Among these, two correspond to a more systematic and fundamental approach.

- The austrian group at LLB was one of the first to undertake an understanding of the sintering mechanisms. Their recent results concern nanocrystalline Y_2O_3 powders : the behaviour, summarized as variation of the total surface of pores (deduced from the Porod law in SANS) versus the volume fraction of porosity, was found very different from that of conventional micrometre-sized powders. Two successive stages are distinguished; in the first one, the surface of irregularly-shaped pores is reduced by surface diffusion, at nearly constant porosity; the second one corresponds to a reduction of total pore volume by transport of vacancies towards the external surface.
- Since 1997, a research programme was undertaken at LLB by the Section de Recherches en Métallurgie Physique of CEA/Saclay, on reactive milling and sintering. The first study concerns the composite material Ag-SnO_2, which is developed for electrical connections applications (PhD thesis of N. Lorrain). Neutron scattering allowed to follow separately the thermal evolution of different types of porosities (using wetting techniques), and the size of Ag and SnO_2 particles during the sintering process. This evolution could be correlated with the formation of small cavities filled with gas, and their subsequent connection in channels at higher temperature.

2.6. Ageing of materials

Nanometer-sized precipitates dispersed in ductile metallic alloys, generally increase the hardness of the materials. A major drawback is the reduction of fracture toughness : this embrittlement, which may appear during ageing in operating conditions, raises safety problems in nuclear industry.

In this context, within the last decade, the thermal or irradiation-induced ageing of materials of nuclear interest has been the object of several studies at LLB by SANS : in many cases, this is the technique which displays the largest scattering contrast between matrix and precipitates; moreover, in the case of (ferromagnetic) steels, supplementary information is obtained from the magnetic interaction with the neutron. We shall mention here the main results obtained in the last two years by CEA and by the german team of Forschungzentrum Rossendorf.

The CEA programme in this field is the object of a collaboration between LLB, the Service de Recherches Métallurgiques Appliquées (SRMA, CEA / Saclay) and the Laboratoire des Solides Irradiés (LSI, CEA / Ecole Polytechnique, Palaiseau).

A new research programme started in 1996 on the ageing of low activation martensitic steels for the fusion reactors (ITER programme). SANS measurements performed at LLB under magnetic field on thermally-aged samples, allowed to characterize the precipitation of carbides (undetected by Transmission Electron Microscopy), and showed a direct correlation between the observed number density of precipitates and the hardening of the material. Furthermore, the stability under neutron irradiation was found to be strongly dependent of the chromium content in the alloy, some of the samples showing an accelerated coherent phase separation of the b.c.c. ferrite into an iron-rich (α phase) and a chromium-rich (α' phase) components (see highlight).

Two austeno-ferritic samples taken on valves situated on the primary circuit of the PWR nuclear reactor of CHOOZ-A, which operated 140 000 hours respectively at 301°C (hot pipe) and 266°C (cold pipe), were studied by SANS, and showed α-α' phase separation in the ferrite responsible of a strong embrittlement; surprisingly, the cold pipe showed a larger phase separation than extrapolated from laboratory ageing tests (= 30 000 hours).

Neutron-irradiated surveillance specimens of Russian VVER-440 type nuclear power plants were investigated and carefully analyzed by SANS at LLB by a German team (Forschungzentrum Rossendorf). The volume fraction of the nanoscaled defects was shown to increase with the neutron fluence, whereas their size distribution (1 to 4 nm) does not change. After post-irradiation annealing, one observes both coarsening and dissolution of the nanoscaled defects. By comparing the ratio of magnetic and nuclear scattering with ASAXS (Anomalous Small-Angle X-ray Scattering) and APFIM (Atomic Probe - Field Ion Microscopy) results, it could be shown that the irradiation-induced defects are clusters consisting of vacancies and different alloying atoms like Mn, Cu and Si in the case of commercial heats, but mainly vanadium carbide in the case of laboratory heats.

2.7. Thin films and multilayers

The major use of neutron reflectivity is in the field of magnetism (with polarized neutrons) and in soft matter. For non-magnetic and non-organic materials, X-ray reflectometry is the usual technique. Nevertheless, neutrons are

useful in the case of favorable contrast : e.g. multilayers or thin films containing titanium, which has a negative scattering length.

This is the case of SiO_y / TiO_x bilayers deposited on glass to optimize solar light transmission properties. A study performed with Stazione Sperimentale del Vitro (Murano, Italy) allowed to obtain much more information (i.e. thickness, roughness, composition) than spectrophotometry, and therefore to calculate the light transmission with improved precision.

The collaboration with Société CILAS on the behaviour of Ti-Ni supermirrors under neutron irradiation finished in 1997 (PhD thesis of K. Nguy). The neutron reflectivity data show that the supermirrors on boron glass cannot be guaranteed after a neutron dose of 3 10^{19} n.cm^{-2} (decrease of 30 % of the reflectivity), which corresponds to 8 years for the core side of the reactor beam holes of Orphée (which see a flux of ~ 10^{11} n.cm^{-2}.s^{-1}), and 80 years at the outlet of the beam holes (i.e. beginning of the guides, flux : ~ 10^{10} n.cm^{-2}.s^{-1}). For the HFR (ILL, Grenoble), because of the higher flux, these numbers are reduced respectively to 1 and 11 years.
Moreover, it was also shown that the boron glass substrate itself deteriorates, by formation of He bubbles.
In conclusion, for the installation of supermirrors at the entrance of the guides, a solution with a metallic substrate, which would offer also better thermal exchanges, should be tested.

In a more prospective direction, we could observe for the first time in non-specular reflectivity diffraction lines from micrometric periodic gratings realized on nickel films. This opens new perspectives for the study of magnetic nanostructures in the plane of thin films, through polarized neutron reflectometry.

2.8 Evolution and Perspectives

Applied research on materials using neutron scattering is expanding, driven by its non-destructive character and the technological needs of society. To meet these needs and promote the neutrons of Orphée by industry, LLB, with the help of its funding organisms (CEA and CNRS), is establishing a new strategy : marketing documents and web page, meetings and workshops, new internal organization. Two meetings have been recently organized in Saclay on the industrial applications of neutrons : a french-italian workshop (in january 1999), and an internal CEA workshop (in june 1999).
We intend also to put in place a new fast access procedure for testing and rapid characterization of samples (in particular in the field of powder diffraction); this is foreseen for the end of 1999.

It is of course important to upgrade the experimental facilities. With a financial participation of INFM (Italy), the stress spectrometer is being equipped with a testing machine that enables strain scanning under constant load (up to 25 kN), constant strain rate or fatigue cycles. The texture diffractometer will be improved with a furnace for in situ measurements and a multidetector to reduce the acquisition time.

From the fundamental point of view, we intend to develop the following subjects in the next years :

- in situ investigation by neutron diffraction (during thermal treatment and/or applied load) of the structure, microstructure and internal stresses in composite materials, with emphasis on line profile analysis *(University of Wien, LLB, University of Reims-Champagne Ardenne, and INFM)*;
- fundamental understanding of the microstructure and texture evolutions of a model two-phase material (50-50 austeno-ferritic steel) during deformation and recrystallization *(International Programme involving LMS/Orsay, LLB, and the Institute of Metallurgy and Materials Science of Krakow)*;
- correlation between milling conditions and microstructure of Giant MagnetoResistive nanocomposite materials (such as (Co, Fe) Cu) *(PhD thesis of S. Galdeano, LLB and CEA / SRMP, Saclay)*;
- SANS study of the influence of irradiation on spinodal decomposition (i.e. α-α' phase separation in b.c.c. Fe-Cr solid solution) *(LSI / Palaiseau and LLB)*.

Future trends in the field are the following :

- enlarged realization of "in situ" experiments;
- coupling with numerical simulations of the behaviour of materials, one major objective of the neutron experiments being the validation of models or codes;
- study of non-metallic materials : e.g. microstructure and ageing of cements;
- development of the study of materials of geological interest : the problems here are very similar to those encountered in metallurgy, with a predominant role of thermomechanical history on the microstructure.

ISOTOPIC ORDERING IN ADSORBED HYDROGEN MONOLAYERS

M. Bienfait[1], J.M. Gay[1], P. Zeppenfeld[2], O.E. Vilches[3], R. Ramos[3], I.Mirebeau[4], G. Coddens[4]

[1]CRMC2, Université de Luminy, Marseille, [2]University of Linz, Linz, Austria
[3]University of Seattle, Seattle, USA; [4]Laboratoire Léon Brillouin (CEA-CNRS)

The mass difference between the molecular isotopes hydrogen (H_2), deuterium hydride (HD) and deuterium (D_2) leads to very different liquid-vapor critical and liquid-vapor-solid triple points in both three and two dimensions. This effect is due to the importance of the zero point kinetic energy in these quantum systems. The zero point kinetic energy also manifests itself in the freezing of binary isotopic mixtures by the observation of bulk quantum fractionation, i.e. the separation at freezing of a liquid rich with the lower mass isotopic molecule, and a solid rich in the larger mass isotope.

The same quantum mass effect should also induce an isotopic ordering at low temperature in the bulk solid phase. Isotopic phase separation was predicted a long time ago by Prigogine[1]. It was observed for ^{3}He-^{4}He mixtures but never for isotopic hydrogen solid solutions, although it has been predicted to occur at temperatures as high as ≈ 4K.

Isotopic phase separation should be expected also in an adsorbed single layer of an isotopic hydrogen mixture. The reduced dimensionality and coordination number in a monolayer with respect to its three-dimensional counterpart makes the relative contribution of the zero-point kinetic energy to the total energy larger than in bulk. This is responsible, among other things, for a substantial difference in the molar areas of H_2 and D_2 at solidification and at monolayer completion. The difference in molar areas lifts the chemical equivalence of the isotopes and can be the driving force which may lead to phase separation.

This was the major motivation of our work on binary mixtures $H_{2(x)}$-$D_{2(1-x)}$ or $HD_{(x)}$-$D_{2(1-x)}$ of the hydrogen isotopic molecules H_2, D_2 and HD adsorbed on graphite, searching for the possible fractionation at solidification and for the expected isotopic phase separation in the solid phase at lower temperature[2-4]. Neutron scattering is well suited for such investigations, taking advantage of the large difference in the coherent and incoherent cross sections of the various hydrogen isotopes. Indeed, the contribution to a diffraction process of all three isotopic molecules is large since the coherent scattering length of both H (b_H = -3.742fm) and D (b_D = +6.674fm) are comparable in magnitude. On the other hand, the large incoherent scattering length of H (especially in the HD molecule which does not undergo ortho-para conversion at low temperatures) is particularly useful in quasielastic neutron scattering measurements.

We performed three kinds of neutron scattering experiments at various hydrogen surface densities (ρ), molar isotopic concentrations (x) and temperatures (T) :

-Diffraction experiments were performed on H_2-D_2 mixtures to identify long range ordering in the solid phases and its possible evolution with temperature.

-Small angle neutron scattering (SANS) investigations were carried out on monolayer H_2-D_2 mixtures. SANS is sensitive to the temperature dependence of the short and medium range structural and compositional order within the mixture. We were thus looking for small clusters of D_2 and H_2.

-Quasi-elastic neutron scattering (QENS) experiments were performed on HD-D_2 mixtures to determine the self-correlation function of the HD molecules in the fluid phase at high temperature (15...30K) and hence the corresponding diffusion coefficient.

The major part of the experiments was performed at the LLB on G6.1 and MIBEMOL ; it was complemented by measurements at the ILL on D1B and D16.

The diffraction measurements mapped portions of the ρ, T, x parameter space. The most meaningful results stem from intensity measurements of the (10) diffraction line at low temperature because they can distinguish between a compositionally disordered adlayer (random mixture) according to

$$I \propto [x b_H + (1 - x) b_D]^2 \qquad (1)$$

and a fully phase-separated system, as given by

$$I \propto x b_H^2 + (1 - x) b_D^2 \qquad (2)$$

The calculated intensity is represented in Fig. 1 (full line) for the random mixture ; it reaches zero for x = 0.64 as a result of the opposite signs of b_H and b_D, respectively. The dashed line represents eq. 2, i.e. the fully phase-separated system.

Two sets of experimental results are reported in Fig. 1, as well. One, for coverage ρ = 1, corresponds to the so-called commensurate $(\sqrt{3}\times\sqrt{3})R30°$ structure. The intensities of the (10) lines fit very well the

calculated intensities of a compositionally disordered mixed crystal. The commensurate solid remains a random mixture down to 3K.

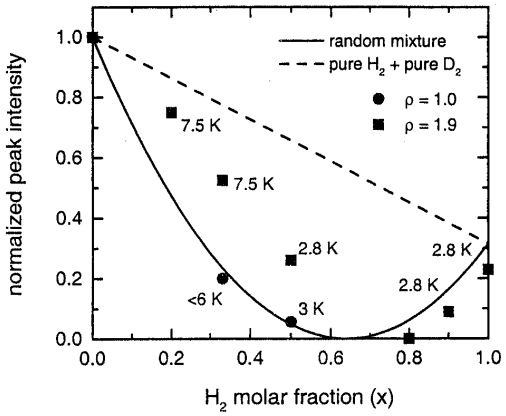

Figure 1. Behaviour of the (10) adlayer diffraction peak intensity

The other coverage ρ = 1.9 corresponds to a complete, very dense, incommensurate monolayer (ρ ≈ 1.5) with, in addition, 30% of a second adsorbed layer (other experiments, not reported here, for ρ ≈1.5, look qualitatively the same). In that case, the measured intensities for 0.2< x < 0.5 are intermediate between the calculated intensities of a random mixture and a fully phase-separated system. Hence, a partial phase separation is observed at monolayer completion for these isotopic molar concentrations.

The small clusters of D_2 or H_2 should be observed by SANS. We have measured the variation of the SANS intensity from 20 to about 3K by decreasing the temperature step by step for x = 0.5 and 4 coverages (ρ = 1.92, 1.54, 1.2 and 1.0). The results are represented in Fig. 2 as the difference of the recorded intensity at 3K, I(3K) and at 20K, I(20K), in order to eliminate the contribution of the beam adsorption due to the hydrogen condensation on the graphite surface.

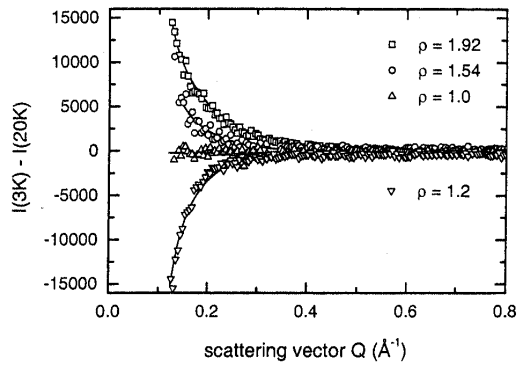

Figure 2 SANS results

At ρ = 1.92 and 1.54, we measure at low temperature an increase of the intensity at small scattering vector which is readily interpreted as the signature of an isotopic clustering in the mixture. Hence, the trend towards phase separation observed by diffraction is confirmed by SANS for these coverages.

The interpretation of the decrease of the SANS intensity at low temperature, observed for ρ = 1.2, is not as straightforward. It suggests that more ordering occurs in the adsorbed layer at low temperature. This is also suggested by diffraction measurements because a superstructure peak is observed for this coverage at 3K.

In the vicinity of the commensurate solid (ρ = 1), the SANS intensity is essentially constant between 20 and 3K. No change in the ordering is detected between these temperatures ; this means that the adsorbed layer remains compositionally disordered down to 3K, as already seen by diffraction measurements.

At higher temperature, in the solid-liquid transition range, we looked, by QENS, for a possible ordering or phase separation at freezing in an isotopic hydrogen mixture adsorbed on graphite. We did not observe any indication of fractionation during the layer solidification but instead a rather unexpected effect : by substituting one half of HD by the heavier molecule D_2 in an adsorbed monolayer, we measured an enhancement of the hydrogen mobility with respect to the pure HD layer in the fluid phase just above the melting temperature. This effect is represented in Fig. 3. It can be interpreted in terms of a strengthening of the bonding of the lighter molecule, resulting from its larger quantum motion. Indeed, the lighter molecule has a larger vibrational amplitude and it tends to experience more strongly the repulsive part of the Van der Waals potential ; this effect stabilizes the lighter isotope adlayer.

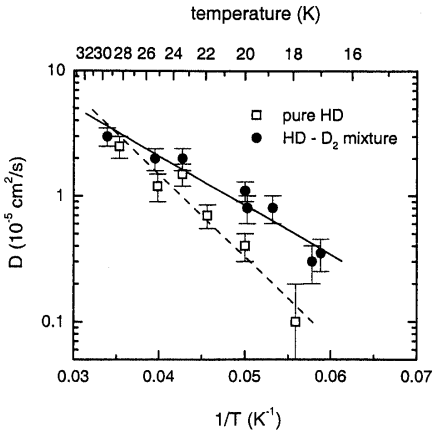

Figure 3. Diffusion coefficient of HD molecules deduced from QENS results

[1] I. Prigogine et al., Physica **XX**, 383 (1954) ; ibid 516 ; ibid 633.
[2] M. Bienfait, P. Zeppenfeld, L.J. Bovie, O.E. Vilches and H.J. Lauter, Physica B **234-236**, 159 (1997).
[3] M. Bienfait, J.M. Gay, P. Zeppenfeld, O.E. Vilches, I. Mirebeau and H.J. Lauter, J. Low Temp. Phys. **111**, 555 (1998).
[4] M. Bienfait, P. Zeppenfeld, R.C. Ramos, J.M. Gay, O.E. Vilches and G. Coddens, Phys. Rev.B (accepted)

ICOSAHEDRAL CLUSTERS AND NON UNIFORM MAGNETISM IN LIQUID PRECURSORS OF AlPdMn QUASICRYSTALS

V. Simonet[1], F. Hippert[1], H. Klein[2], M. Audier[2], R. Bellissent[3]

[1]Laboratoire de Physique des Solides , Université Paris-Sud, 91405 Orsay Cedex, France
[2]L.T.P.C.M, E.N.S.E.E.G., B.P.75, 38402 Saint Martin d'Hères, France
[3]Laboratoire Léon Brillouin (CEA-CNRS)

In a recent study of liquid AlPdMn alloys[1] leading to quasicrystalline or approximant phases by primary crystallisation[2], we put onto light a very strong local order. The close similarity between the intense Bragg peaks of the solid phase and the main peaks of the liquid structure factor suggests an icosahedral local order. On the other hand the liquid shows up a paramagnetic behaviour whereas the solid phases are non magnetic. The magnetic susceptibility of the liquid is proportional to the Mn content of the AlPdMn alloys ; it increases with increasing temperature, which could be associated to a decrease of the amount of icosahedral clusters[3].

Most structural models for quasicrystals involve packings of various icosahedral clusters with a large number of atoms, such as Mackay clusters (54 atoms) in AlPdMn quasicrystals or Bergman clusters (104 atoms) in AlLiCu quasicrystals. The same clusters are also found in the approximants of quasicrystals, which are periodic phases with large unit cells whose structures are closely related to that of quasicrystals. Clusters are not only a convenient geometrical description of these complex phases, but can also play a role in their properties. In the case of a liquid - icosahedral solid phase equilibrium, it might be expected that the local order in liquids forming quasicrystals reflects the local organization of atoms in the solid. Therefore we have undertaken simultaneously a simulation of the liquid local order based on icosahedral clusters and an extension of our experimental work up to higher temperatures and with several Mn compositions. Polarised neutrons have been used to investigate the Mn magnetic form factor in the liquid.

Neutron diffraction

Neutron scattering spectra measured on 7C2 spectrometer on the $Al_{72.1}Pd_{20.7}Mn_{7.2}$ alloy at 1143 K where the eutectic was molten (and hence the solid icosahedral phase coexisted with a small fraction of liquid) and at 1223 K just above the melting point (T_L=1160 K) are shown in figure 1. The broad maxima of the differential scattering cross-section in the liquid state correspond to the main Bragg peak groups of the icosahedral phase. At small Q values in the liquid state, a paramagnetic contribution is superimposed to the measured structure factor as explained later.

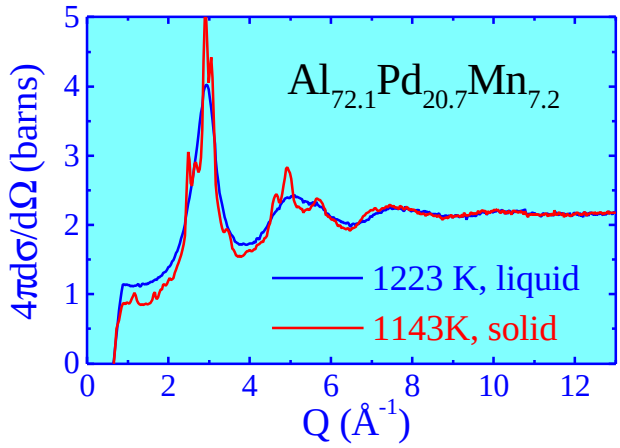

Figure 1. Structure factor of AlPdMn alloys in the solid state (just below the melting point) and in the liquid state (just above the melting point), measured on 7C2, LLB.

The similarity between the liquid and solid spectra extends up to the largest Q values. The same kind of observation holds for other studied alloys : $Al_{77}Pd_{18}Mn_5$ and $Al_{76.5}Pd_{20}Mn_{3.5}$. Such an observation suggests the presence of strong local order in the liquid state above T_L, reminiscent of that in the solid.

We have therefore searched for a possible evolution of the neutron scattered intensity with increasing temperature in the liquid state. This study was performed up to 1923 K, using the spectrometer D4B at ILL, on the $Al_{72.1}Pd_{20.7}Mn_{7.2}$ alloy whose primary crystallization gives rise to the largest proportion of icosahedral phase. Results are shown in figure 2.

As expected in liquid metallic alloys, the oscillations of the structure factor are broadened and their amplitudes decrease with increasing temperature.

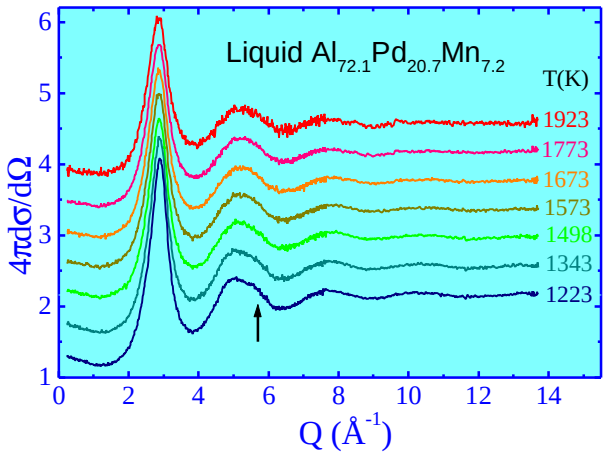

Figure 2. Differential neutron scattering cross-section versus temperature for the $Al_{72.1}Pd_{20.7}Mn_{7.2}$ in the liquid state (measured on D4, ILL). The vertical scale corresponds to the data measured at 1223 K. The curves at successive temperatures have been shifted by steps of 0.5 barns.

An evolution of the liquid structure is suggested by the fact that the second peak shoulder (shown by an arrow around 5.5 $Å^{-1}$), well defined just above the melting point, is progressively damped with increasing temperature. Simultaneously the low Q limit of the intensity increases which indicates an increase of the magnetic moment. Finally it must be emphasized that the oscillations at larger Q remain well defined up to 1923 K and **their position is unchanged**, while the position of the first peak shifts towards small Q as expected from thermal expansion.

Polarized neutron scattering

Polarized neutron scattering experiments were performed on the D7 spectrometer at ILL (Grenoble) at room temperature and at 1170 K, just above the liquidus temperature[4]. Incident neutrons were sequentially polarized along the three perpendicular directions. For each direction of polarization, the spin-flip and non-spin-flip scatterings were alternately measured. Paramagnetic and nuclear spin incoherent scatterings give rise to both spin-flip and non-spin-flip processes, while the nuclear coherent and incoherent (isotopic and chemical) scatterings are non-spin-flip. By suitable combinations of the measured spin-flip and non-spin-flip signals, the contributions of the nuclear spin incoherent scattering, the nuclear scattering and the paramagnetic scattering can be determined. The differential magnetic scattering cross-sections at 300 K and 1170 K (obtained by averaging spin-flip and non-spin-flip measurements) are shown in Figure 3. Very large error bars are due to small counting rates resulting from the significant attenuation of the incident and scattered beams within the neutron polarizer and analyzer devices. Nevertheless, in agreement with previous results, a paramagnetic scattering is detected in the liquid state, while it is not measurable in the solid state. The differential nuclear scattering cross-section has been extracted as well it ascertains that the chemical incoherent scattering increases on melting and reaches its maximal value in the liquid state above T_L. Thus the increase of the differential scattering cross-section measured with unpolarized neutrons on melting is not only due to the onset of paramagnetic scattering in the liquid, but also to an increase of the chemical incoherent scattering.

Knowing the chemical incoherent scattering contribution, the differential paramagnetic scattering cross-section in the liquid can be calculated from the differential scattering cross-section measured using unpolarized neutrons. In the $Al_{72.1}Pd_{20.7}Mn_{7.2}$ alloy, at 1223 K, from $\sigma_0 = 1.2 \pm 0.06$ barns at Q = 0.2 $Å^{-1}$ one obtains $4\pi(d\sigma/d\Omega) = 0.49$ barns which is much larger than the signal measured using polarized neutrons ($\cong$ 0.075 ± 0.015 barns). This discrepancy is probably due to the quasi-elastic nature of the paramagnetic scattering. On D7 the integration on energy is limited, on the neutron energy loss side, by the low incident neutron energy (E_i =3.5 meV) and, on the neutron energy gain side, by an effective cut-off (around 10 meV) due to the progressive decrease of the efficiency of the neutron spin analyzers with increasing energy.

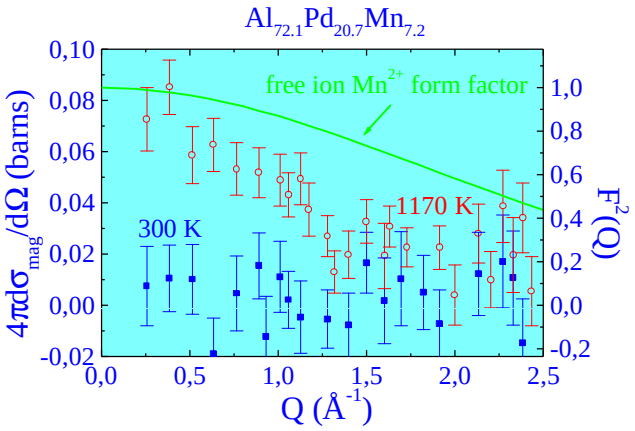

Figure 3 . Polarized neutron scattering measurements performed on D7, ILL : Q dependence of the differential paramagnetic scattering cross-section in $Al_{72.1}Pd_{20.7}Mn_{7.2}$ at 300 K (full blue squares) and at 1170 K in the liquid state (open red circles). There is a paramagnetic scattering in the liquid state and no such signal in the solid state. The data in the liquid state, normalized to 1 at Q=0 (right vertical scale), are compared to the form factor of a free Mn^{2+} ion (solid line).

On the contrary, the high incident energies used on the 7C2 and D4B spectrometers ($E_i \cong$ 170 meV) permit an integration of a much larger fraction, or almost the whole, of the paramagnetic response.

Assuming the whole signal is integrated on 7C2 and D4B, then only 15% of the paramagnetic signal was detected on D7 at 1170 K. However, even with such a poor precision in the data, one can observe a narrowing of the form factor compared to that of the Mn^{++} ion, which suggests strong magnetic correlations in this liquid alloy.

Icosahedral local order of the liquid state

The great similarity found between the structure factor of the liquid AlPdMn alloys and the diffraction spectrum in the solid quasicrystalline phase led us to assume the presence of a strong local icosahedral order in the liquid. In order to ascertain this hypothesis, we analyze more quantitatively the liquid structure factor through numerical simulations based on icosahedral clusters.

Although simulations of the measured structure factors in the whole Q-range are a very complex task, an analysis of the structure factor at large Q is possible under several conditions and indeed brings very interesting information on the local order. The principle of the method, initially introduced to describe molecular solids, implies that a cluster can be defined in the liquid and that the atoms within the cluster are much more rigidly bound together than to other atoms in the system. The structure factor can be written as :

$$S(Q) = \frac{1}{N_{at}^{c}\left\langle b^{2}\right\rangle}\sum_{i,j=1}^{N_{at}^{c}} b_i b_j \frac{\sin Qr_{ij}}{Qr_{ij}} e^{-W_{ij}}$$

It is compared to the experiment on figure 4a.

Because of the similarity between local order in the icosahedral solid and in the liquid, the choice of the cluster was guided by the structural description of several AlMn and AlPdMn approximant phases. We assumed therefore an icosahedral cluster of Al centered on a Mn Atom[6]. The first icosahedron edge Al-Al distance $<r_1>$ was taken equal to 2.6 Å and the mean square variation $<\delta r_1^2>$ of this distance was 0.015 $Å^2$ as expected from the results of structure refinement of solid phases. $<r_0>$ is the Mn-Al distance (see insert of the figure 1b). The other icosahedron distances are then fixed. Their mean square variation can be obtained assuming that : $<\delta r_i^2> = <\delta r_1^2> (<r_i> / <r_1>)^2$.

The Debye-Waller term is then defined with: $W_{ij} = <\delta r_i^2> / 3$.

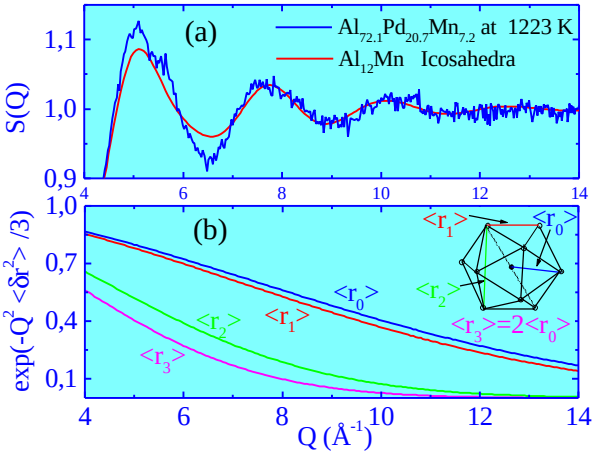

Figure 4.(a): Comparison for Q > 4.5Å^{-1} of the measured structure factor at 1223 K in $Al_{72.1}Pd_{20.7}Mn_{7.2}$ (blue) with the calculated structure factor assuming $Al_{12}Mn$ icosahedra (red solid line)
(b) Q dependence of the Debye-Waller factors for the four pair distances within the $Al_{12}Mn$ icosahedron

Conclusion

In this work, by using a cluster based numerical simulation, we have proven the existence of **icosahedral clusters** with lifetime greater than the typical neutron interaction time with the cluster (i.e. 10^{-10} seconds).

The existence of such clusters with the same geometry up to very high temperatures, is the signature of a **molecular type** local order in a liquid **metallic alloy**.

Moreover this liquid is **non homogeneous** as far as no change occurs in intracluster distances, while bulk density strongly decreases.

We have shown that the unexpected behaviour of the magnetic properties of these alloys can be understood under the assumption than **Mn becomes magnetic outside of the $Al_{12}Mn$ clusters**.

References

[1] D.Shechtman, I.Blech, D.Gratias, and J.W. Cahn, Phys. Rev. Lett. **53**, 1951 (1984).
[2] M. Audier, M. Durand-Charre and M. de Boissieu, Phil. Mag. B **68**, 607 (1993).
[3] F. Hippert, M. Audier, H. Klein, R. Bellissent, D. Boursier, Phys. Rev. Lett. **76**, 54 (1996).
[4] O. Schärpf and H. Capellman, Phys. Stat. Sol. (a) **135**, 359 (1993).
[5] H. Klein, L. Descotes, M. Audier, R. Bellissent, and F. Hippert, J. of non Cryst. Solids **205-207,** 6, (1997)
[6] V.Simonet, F. Hippert, M. Audier, H. Klein, R. Bellissent, H.Fischer, A.P.Murani, D.Boursier, Phys. Rev. B **58**, 6273 (1998).

RESIDUAL STRESSES AND HARDENING NEAR CRACK TIP REGIONS OF AUSTENITIC STEEL FATIGUE SPECIMENS.

K. Hirschi[1], M. Ceretti[1], B. Marini[2], J.-M. Sprauel[3]

[1.] Laboratoire Léon Brillouin (CEA-CNRS)
[2.] CEREM/SRMA, CEA-Saclay, 91191 Gif sur Yvette Cedex
[3.] Laboratoire MécaSurf, ENSAM, 2 cours des Arts et Metiers, 13640 Aix en Provence

Austenitic stainless steel 316L is used extensively in the field of nuclear industry, and more specifically in the primary circuit of fast breeder reactors. As the normal operation temperature of the latter is about 650°C, it is very important to determine the role of residual stresses in the deformation and the fracture process in order to estimate the component's lifetimes. The plastic deformation is also an important parameter related to the residual stress relaxation and its redistribution after fatigue loading.

The aim of this work was to determine the residual stress field in cracked fatigue specimens of austenitic stainless steel 316L by neutron diffraction techniques in order to use this data for quantifying the influence of the different loading parameters on the fatigue crack growth. On the other hand, some microstructural parameters, such as the average size of coherently diffracting blocks D and the mean-square microstrain $<\varepsilon^2>^{1/2}$, were estimated by combining neutron and X-ray (synchrotron radiation) diffraction techniques. In fact, the shape and the broadening of diffraction profiles are directly correlated with the evolution and redistribution of microstructural defects .

Non-destructive neutron diffraction technique is nowadays extensively used for the determination of **internal elastic stresses** in polycrystalline materials due to the homogeneous distribution of strains across several grains, which result in a shift of the angular position of the Bragg peaks. However, the analysis of **plastic strains**, due to microstructural defects, by neutron scattering investigations still remains quite rare, in contrast to X-ray diffraction, widely used for this kind of analysis. Nevertheless, due to the high penetration of neutrons in most materials, the neutron diffraction is the only non-destructive technique, which enables to get information within a defined volume in a bulk sample and not only limited to the surface (as in the case of X-rays).

For the analysis of plastic strains by neutron scattering, experimental and theoretical methods for neutron diffraction line broadening analysis were developed [1]. These methods generally require a high instrumental resolution, which has been achieved by optimising the experimental conditions (large monochromator take-off angle and small incident beam divergence) [2]. Additionally, a new method of single peak analysis with indirect deconvolution of instrumental profile was developed to relate the diffraction profile parameters with the microstructural parameters.

Measurements were performed on two Crack Test (CT) specimens of austenitic stainless steel 316L (Fig. 1) subjected to fatigue cycling with different load ratio (R) in order to modify the dimensions of the plastic region close to the crack tip (R=0.1 and R=0.5), called in the following CT_1 et CT_2, respectively. In particular, the first sample, with R=0.1, had been subjected to 25750 fatigue cycles, while the second one (R=0.5) has been submitted to 19530 cycles. A third specimen (CT_3) was deformed by tension up to 5 mm crack opening.

1. Internal elastic stresses

In the first part of the work, we have studied the macroscopic residual stresses by neutron diffraction. Three dimensional strain measurements (x, y, z directions) were performed in the middle of the sample, along the crack opening direction y, on the "strain dedicated" G5.2 diffractometer of the LLB.

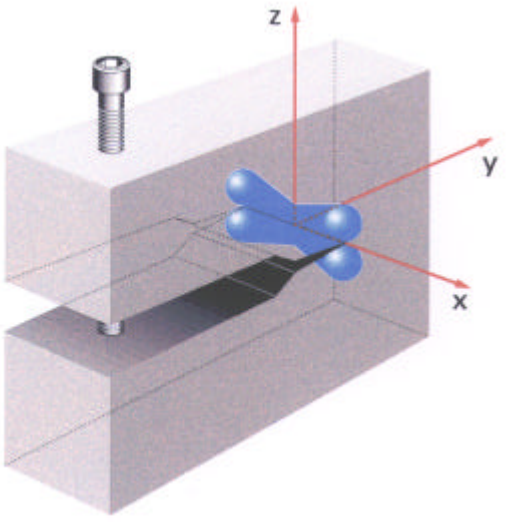

***Figure 1**: Geometry of the CT samples and measurements directions. The plastic zone near the crack tip is schematised in blue. The samples were 70 mm long in the direction of the crack growth, 45 mm high and 10 mm thick. Neutron measurements have been performed in the middle of the sample (at a depth of 5mm), along the crack opening direction y.*

For all the investigated specimens, a three dimensional stress state was observed. In particular, the residual stresses obtained for the sample with a small R (CT_1) are rather weak and they increase in the second sample (CT_2) with higher R. Experimental residual stress distribution along the crack opening direction for the third sample (CT_3) is shown in figure 2, together with a finite element calculation. As seen from the figure, the maximum stress level was observed at 2 mm from the tip, where σ_{xx} = 300 MPa, σ_{yy} = 500 MPa and σ_{zz} = 800 MPa. At the distance of 8mm from the tip, the σ_{xx} and σ_{yy} components were found to be very low, whereas the σ_{zz} component becomes large and compressive. These measurements show a good agreement with a finite elements (3 dimensional) calculation performed using CASTEM2000 code, developed at DEMT (CEA). A small disagreement between the experimental and theoretical results was observed essentially in the region of some mm near the crack tip. This can be explained by the different spatial resolution used in the neutron measurements. In fact, the size of the finite elements selected in the calculations was 0.187 mm near the crack and 1.275 mm at the edge of the sample, while the spatial resolution ("gauge volume") of neutron measurements was 1x1x1 mm^3. We note as well that the calculated values of stresses are slightly higher than measured ones. This is probably due to relaxation effects due to the plastic deformation induced by the tensile test. Another possible reason for the deviation from the maximum value can be due to the fact that the calculation does not take into account the effect of the crack propagation.

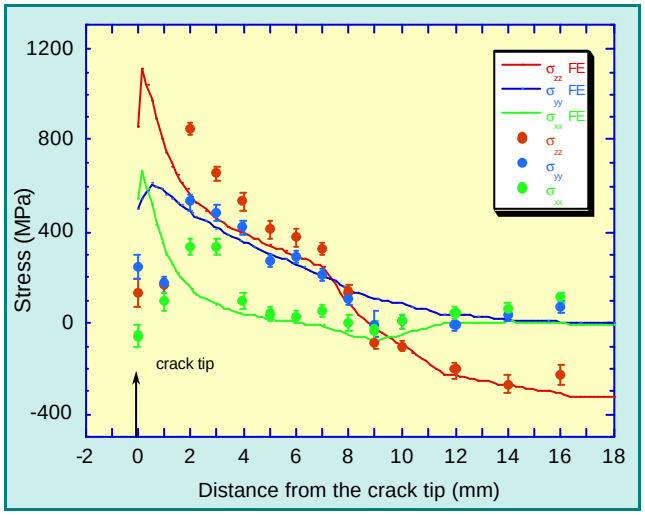

***Figure 2** : Residual stress evolution as a function of the distance from the crack tip of the CT_3 sample. Comparison between the experimental results (dots) and the values obtained by Finite Element calculation (continuous lines).*

2. Plastic strains : neutron measurements

In the second part of the work, the experimental study of microstructure and plastic deformation in the region close to the crack tip was performed by neutron and X-ray (synchrotron) diffraction. In fact, it is important to estimate the dimension of the plastic zone, created around the crack's tip, which is responsible for the stress redistribution affecting the crack propagation.

The microstrains evaluation by neutron diffraction have been performed in the middle of the sample (at a depth of 5mm) using the profile broadening analysis, based on the single-line Keijser's method [1]. The basic assumption of this approach is that the sample broadened profile can be described by the convolution of a Gauss function and a Cauchy function, depending on the strain and size, respectively. The indirect deconvolution method has been developed to extract the instrumental profile from the experimental data. The plastic zone was clearly distinguished for the CT_2 and CT_3 samples with the peak breadth considerably larger than that of reference sample. The dimension of the plastic zone (depending on the directions x, y, z) is about 2 to 3 mm for the CT_2 sample and about 4 mm for the CT_3 sample. The estimation of the plastic deformation and microstructural parameters (D and $<\varepsilon^2>^{1/2}$) was done using a previous calibration on prestrained tensile specimens, by performing neutron single line broadening analysis. For the CT_3 sample it was found that the maximum plastic strain in the directions perpendicular (z) and parallel (y) to the crack propagation is localised at 1mm from the tip and it attains about 30% (Figure 3).

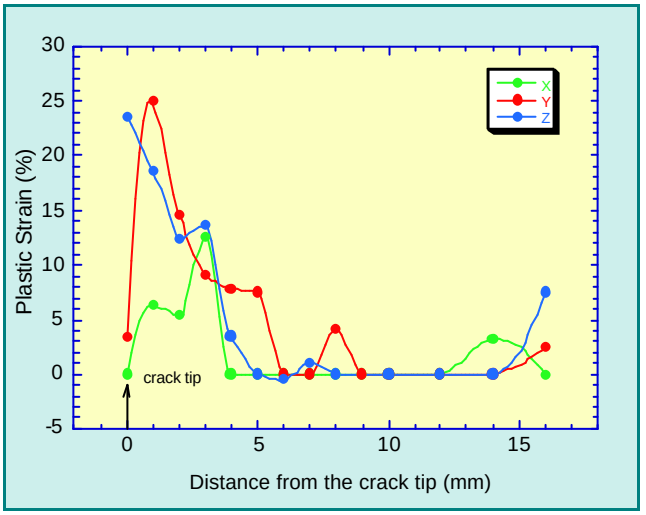

***Figure 3** : Evolution of the plastic strain as a function of the distance from the crack tip, in the sample CT_3, determined by neutron diffraction.*

3. Plastic strains : X-ray measurements

These results, obtained by a single peak broadening analysis, have been completed by a Warren-Averbach analysis using several X-ray (synchrotron radiation) Bragg reflections and higher orders. These complementary measurements were performed at the sample surface on the four circle diffractometer, WDIF4C, installed on the light guide DW22 at L.U.R.E. (Orsay). Plastic strains were determined using a recently developed theoretical model, based on the Warren-Averbach analysis and taking into account the contribution of Elastic Strain Heterogeneity (ESH) of the domains on the profiles broadening [3]. The values obtained for the mean size of the coherently diffracting blocks <L>, the mean square of the 2nd kind micro-strains $\langle\varepsilon_0^2\rangle^{1/2}$ (related to the ESH effects) and the mean square of 3rd kind micro-strains $\langle\varepsilon_1^2\rangle^{1/2}$ are reported in Figure 4 as a function of distance from the crack tip. As seen from the figure, the microstructural parameters obtained are quite scattered. This is probably due to the relatively large grain's size compared to the small X-rays beam dimensions and its weak divergence. In particular, the ESH and size effects are the most visible in the region close to the tip (2-3mm). In the region between 4 mm and 9 mm, we obtain very small (or zero) values of plastic deformation and negative values of <L>. This is due to the imprecision of the deconvolution as the Bragg peak breadth is very close to the instrumental width. The calculated size of coherently diffracting blocks, which is about 255Å at the crack tip, corresponds to plastic strain of 30%. The increase of distortion values at the edge of the sample shows the presence of strong plastic strains in this region.

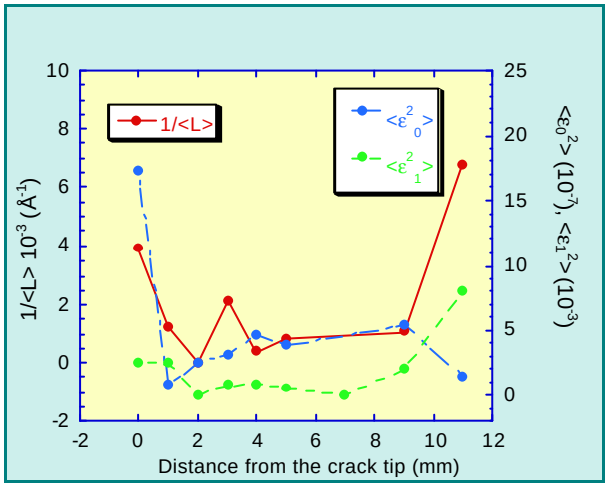

Figure 4 *: Evolution of the diffraction coherent domains size <L>, and of the microstrains $\langle e^2_0\rangle$ (2nd order) and $\langle e^2_1\rangle$ (3rd order) as a function of the distance from the crack trip in the CT_3 sample, determined by Warren-Averbach analysis using synchrotron radiation*

In summary, neutron diffraction has been applied to study the in-depth triaxial stress field and the hardening effect along the crack line in austenitic steel fatigued specimens. For the first time, the plastic zone close to the crack tip has been characterised by the neutron technique using diffraction line broadening analysis [4]. Complementary measurements were made using X-rays (synchrotron radiation) at the sample surface. A quantitative comparison between neutron and synchrotron results is not possible as the ESH is not taken into account in the neutron broadening analysis and the explored regions are not the same.
However, this study has shown that the neutron non-destructive technique, complementary to the X-ray technique, is a powerful tool for mechanical and microstructural characterisation of bulk samples.

References

[1] de Keijser T. H, Mittemeijer E. J., Rozendaal H. C. F., *J. Appl. Cryst*. 16 (1983), 309-316
[2] Hirschi K., Ceretti M., Lukas P., Ji N., Braham C., Lodini A., *Textures and Microstructures*, (1999), in print
[3] Marbelly P., *Contribution à l'étude des pics de diffraction. Approche expérimentale et modélisation micromécanique*, Thèse de Doctorat, ENSAM, Aix en Provence, 1996.
[4] Hirschi K., *Analyse des contraintes résiduelles et des paramètres microstructuraux par diffraction des neutrons dans un acier austénitique inoxydable*, Thèse de Doctorat, Université de Reims, 1999.

"IN SITU" NEUTRON SCATTERING STUDY OF HYDROGEN-CONTAINING ZIRCALOY-4 ALLOYS

F. Couvreur[1], G. André[2]

[1]CEA, DRN/DMT/SEMI/LM2E, CEA-Saclay, 91191 Gif-sur-Yvette cedex
[2]Laboratoire Léon Brillouin (CEA-CNRS)

Aims of the study

The fuel cladding of Pressurized Water Nuclear Reactors (PWR), made in Zircaloy-4 (zirconium-based alloy, containing in weight typically 1.4% Sn, 0.2% Fe and 0.1% Cr), is sensitive to hydrogen absorption in the usual working conditions (i.e. under H_2O at 300°C). Hydride platelets may form, which are an important embrittlement factor of the cladding, and also which induce a swelling when they dissolve in the α-h.c.p. Zircaloy matrix. Moreover, recent studies suggest that these hydrides may be an accelerating factor of corrosion. This aspect will be all the more important as the new working PWR conditions will be more demanding.

It is therefore essential to characterize and understand the mechanisms of hydride formation and dissolution, in particular under neutron irradiation : this is the object of a research programme undertaken by the "Direction of Nuclear Reactors" of CEA, which includes a neutron scattering study at LLB.

The large coherent and incoherent cross-sections of hydrogen make this tool very powerful to determine the hydrogen content and characterize the hydrides ; indeed, the incoherent cross-section gives rise to a continuous background in diffraction spectra, which is **proportional** to the hydrogen content, and is (nearly) independent of scattering angle ; the coherent cross-section contributes significantly to the structure factor of the hydride phase, i.e. to the intensity of its diffraction peaks. Zirconium is a specially favorable element for this study, because its neutron absorption coefficient and incoherent scattering cross-sections are very weak : the diffraction spectra of H-free samples show very low background.

Results

In a first stage, we have shown, on the powder diffractometer G4.1 (equipped with a 800 cell linear multidetector), that the incoherent scattering contribution, obtained from the measurement of the background on samples originating from cladding tubes, allows to determine **non destructively** the total amount of incorporated hydrogen (Fig. 1), with very good sensitivity and precision (< 20 ppm weight). The principle of measurement consists to calibrate in absolute value the incoherent signal measured on a reference vanadium sample of cylindrical shape, after subtraction of the instrumental background ; this allows to calibrate the signal difference between the hydrogenated sample and an hydrogen free sample.

On the other hand, the diffraction peaks of the hydride (f.c.c. δ-ZrH_2) and Laves phase precipitates ($Zr(Fe,Cr)_2$) can be easily detected and analysed, for very weak (< 1% atomic) H, Fe and Cr contents, which is not possible in conventional X-ray diffraction.

In a second stage, we have performed "in situ" measurements at various temperatures (between 20 and 500 °C) under secondary vacuum, on a section of Zircaloy-4 cladding tube containing 642 ppm weight hydrogen (length of the sample : 50 mm, diameter : 9.5 mm). The typical measuring time for a single spectrum was 2 hours. In a single experiment (total duration : 5 days), we have been able to obtain simultaneously from the analysis of diffraction spectra the following informations :

- total hydrogen content,
- hydrogen content in hydride form,
- crystallographic characterization of the $Zr(Fe,Cr)_2$ and ZrH_2 precipitates,
- solubility of H, dissolution of hydrides (Fig. 2),
- influence of H on the thermal expansion of Zircaloy-4 (Fig. 3).

Desorption of hydrogen out of the sample under secondary vacuum was observed above 450 °C, by a decrease of the incoherent background signal.

Conclusions and future prospects

Neutron scattering is the only experimental technique which allows to measure non-destructively the total hydrogen content in Zircaloy tubes. But, more than a simple hydrogen content determination at room temperature, the neutron scattering technique, when combined use is made of the incoherent background and of the diffraction peaks, is also a very rich technique, sensitive and reliable, and quite appropriate to follow "in situ" at high temperature the precipitation/dissolution phenomena of zirconium hydrides, even for very weak contents of precipitates.

Future work will be the examination of neutron irradiated samples in PWR conditions (influence of irradiation on hydrogen solubility and on the structure of precipitates) and the study of the behaviour of the cladding in accidental situation (loss of primary cooling), which will require measurements at higher temperature (≈1000 °C).

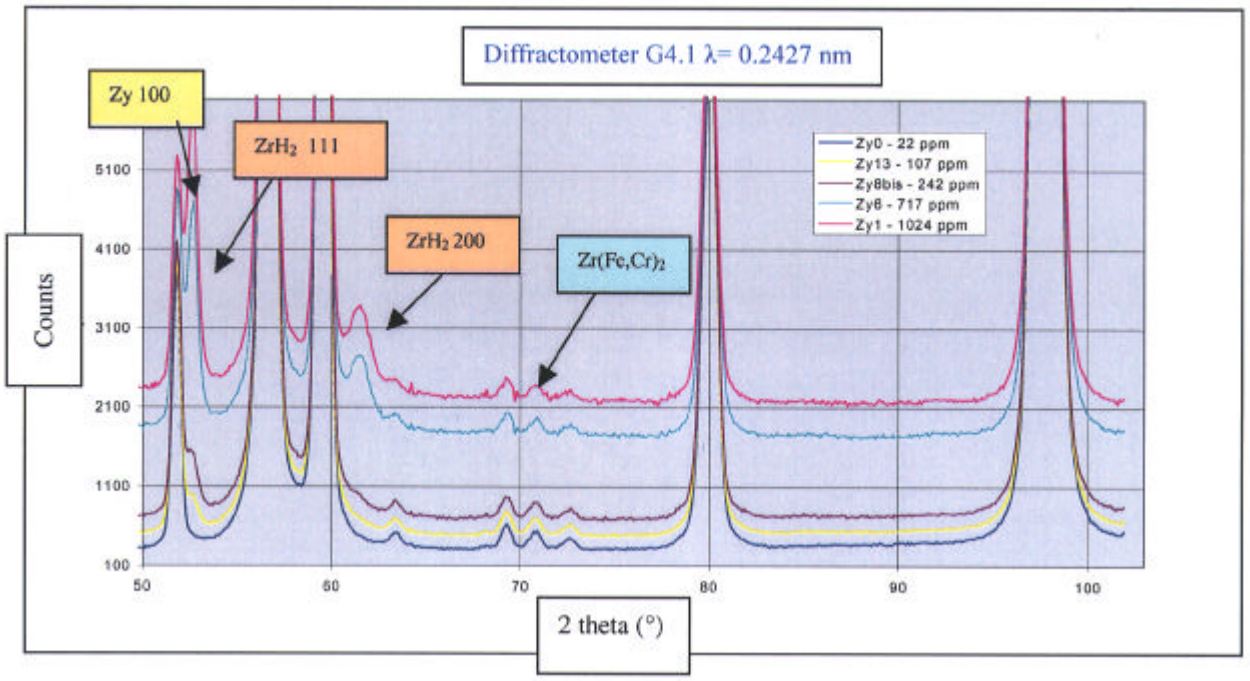

Figure 1 : Powder diffraction diagrams measured for several Zircaloy samples. One observes the increase of background with the hydrogen content, and the weak diffraction lines of δ-ZrH_2 hydride and Laves phase.

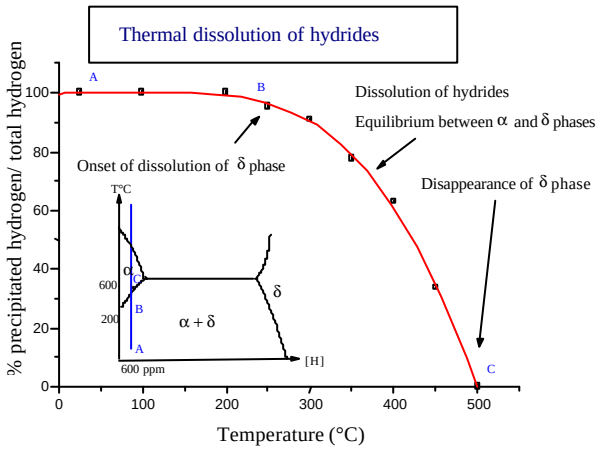

Figure 2 : Proportion of hydrogen content in hydride form (d-phase) versus temperature, for a sample containing 642 ppm weight hydrogen. This quantity decreases with increasing temperature, according to the phase diagram shown in inset : above 500°C, dissolution of the hydrides is complete and the sample is a single-phase Zr-based (a) hexagonal solid solution. It allows to determine the hydrogen solubility curve in the studied material, between room temperature and 500°C, and to deduce a value for the enthalpy of dissolution of the d-hydrides in Zircaloy-4 : DH = 41.5 kJ / mol.

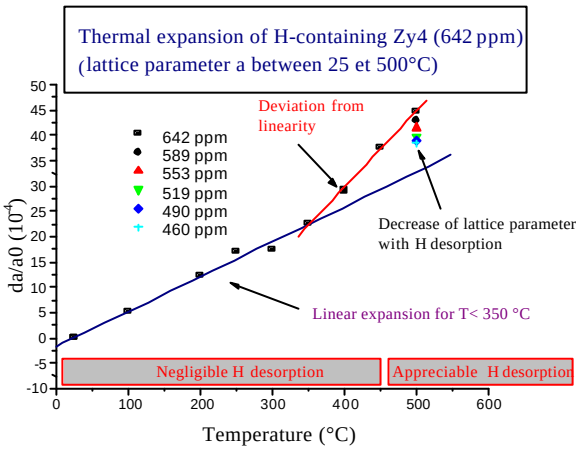

*Figure 3 : Temperature dependence of the lattice parameter **a** of Zircaloy-4 (sample containing 642 ppm weight hydrogen). A similar curve is found for the lattice parameter **c**. We attribute the increase of slope above 350°C to the dissolution of hydrides, which introduces interstitial hydrogen atoms in the a-Zircaloy matrix and a supplementary swelling. This explanation is confirmed by the observed decrease of lattice parameter during an isothermal stay at 500°C, due to hydrogen desorption out of the sample.*

References

[1] P. Wille, D. Bunemann, H.J. Lahann, H. Mertins, « Hydrogen diffusion in metals measured by neutron scattering and adsorption », IAEA SM 219/36, pp.325-338 .

[2] J.H. Root, R.W.L. Fong « Neutron diffraction study of the precipitation and dissolution of hydrides in Zr-2.5Nb pressure tube material » Journal of Nuclear Materials 232 (1996) 75-85.

AGEING UNDER THERMAL TREATMENT OR NEUTRON IRRADIATION OF LOW ACTIVATION MARTENSITIC STEELS

M.H. Mathon[1], G. Geoffroy[2], Y. de Carlan[3], A. Alamo[3], C.H. de Novion[1]

1 Laboratoire Léon Brillouin (CEA-CNRS)
2 Laboratoire des Solides Irradiés, Ecole Polytechnique, 91128 Palaiseau Cedex
3 CEA, DTA/DECM/SRMA, CEA Saclay, F-91191 Gif-sur-Yvette

Low Activation Martensitic (LAM) steels are candidates for internal structures of fusion reactors. The concept of Low Activation steels was introduced in nuclear industry for new materials that offer benefits on maintenance operations and waste management. For martensitic/ferritic steels, the main alloying elements such as molybdenum, niobium and nickel present in commercial steels are substituted by elements such as tungsten, vanadium, manganese and tantalum. These elements have a similar influence on the processing and the structure, but exhibit a lower radiological impact. The assessment of potential reduced activation martensitic steels requires a good understanding of the microstructural features in correlation with the mechanical behaviour. Consequently, much effort is underway to study the microstructural evolutions in these materials occurring under thermal ageing or neutron irradiation, and the effects of the substitution of W to Mo and Ta to Nb.

The microstructural investigations are focused on the following phenomena :
- precipitation of various carbides or nitrides : in particular of $M_2(C,N)$ particles responsible of a "secondary" hardening phenomenon (defined in §1),
- formation of the Laves phases $Fe_2(Mo,W)$ under long thermal ageing around 500°C,
- decomposition by a spinodal mechanism of the ferritic phase resulting in an ultra fine-scale interconnected network of Fe-rich α and Cr enriched α' phases or in very small α' particles around 400°C.

All these microstructural evolutions (which are at the origin of hardening phenomena and embrittlement) were studied in different martensitic steels with a chromium content between 7 and 12 at.%, using Small Angle Neutron Scattering (SANS). Indeed SANS allows, in this kind of materials, to characterise very small precipitates at early ageing time when they are not detected by Transmission Electron Microscopy. This is in particular the case for α-α' decomposition, which introduces very weak contrast for X-rays or electron scattering. Furthermore, the ferritic matrix being ferromagnetic, the A(q) ratio of the magnetic and nuclear contrasts between the matrix and particles gives information about their chemical composition [1].

1. Study of the secondary hardening phenomenon

In quenched (after 1h at 1050°C) and subsequently annealed at 450-550°C materials which simulate the thermally affected zone near a weld, one observes, at relatively short annealing time, an increase of the hardness which is called secondary hardening[2]. It is related to the first steps of Cr-rich M_2X (X= C or N) precipitation; the latter is detected by Transmission Electron Microscopy (TEM), but only after almost 100 annealing hours when the size of the particles is close to 10 - 20 nm. In order to describe the precipitation at the early stage of thermal ageing treatment, SANS experiments were performed on a conventional alloy "T0" (Fe-9%Cr-1%Mo) and on a LAM material "F82H" (Fe-7.5%Cr-2%W), previously aged for various durations at 500°C.
For the T0 alloy, an increase of the SANS intensity is observed at all annealing times. The mean diameter and number density N_p of the M_2X particles deduced from SANS are shown on figure 1. At short ageing time (<5h), the particles size remains small (1 to 2 nm) whereas N_p increases ("nucleation" stage). Around 5h ageing time, N_p and the hardness reach simultaneously their maximum value, corresponding to optimal pinning of the dislocations by the small precipitates. At long ageing time, N_p and the hardness decrease sharply whereas the average precipitate diameter increases by one order of magnitude ("coalescence" stage).

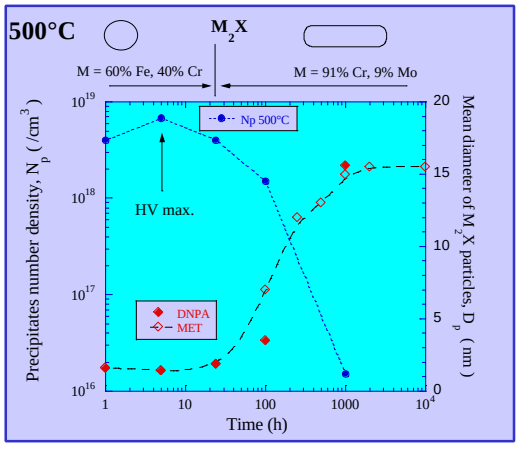

Figure 1 : Evolution with ageing time at 500°C of the mean size and the number density of the M_2X precipitates measured by TEM and SANS in the T0 alloy.

The form factor of the precipitates, obtained from the fit of the SANS curves, is spherical for the shorter

time (t<100 h) and afterwards rod shaped ellipsoidal with a ratio between the big and the small axis of about 3. For large precipitates, the aspect ratio and the mean size measured after 1000 h, are in good agreement with TEM observations.
The A(q) ratio was found to decrease strongly with ageing time (i.e. from 6.6 to 2.4); this could be explained only by a progressive enrichment in Cr and by assuming that the interstitial element X is essentially carbon and not nitrogen. At long ageing time, the A ratio is in agreement with the presence of 9% Mo in the carbides measured by TEM.
For the low Cr content LAM alloy F82H, the maximum volume fraction of the carbides is noticeably smaller than for T0 (0.7% instead of 1.5%); this can explain the very weak increase of the hardness observed in the F82H alloy (figure 2). Besides, the chemical composition of the carbides at long ageing times, consistent with the A value, is 80%Cr-20%V (at. %) : contrary to the case of Mo in the T0 alloy, W does not enter in the composition of the M_2C carbides.

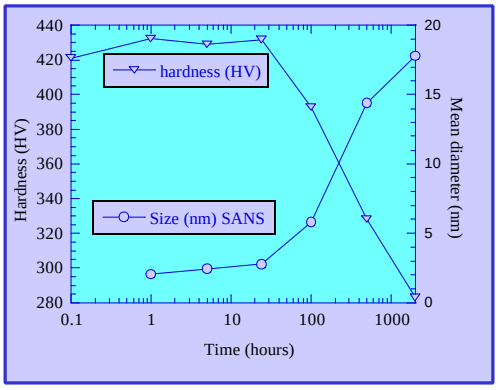

Figure 2 : Evolution with ageing time at 500°C of the hardness and of the mean size of the M_2X precipitates measured by SANS in the Low Activation F82H alloy.

2. Ageing under long thermal treatment or neutron irradiation

In austenitized (quenched from high temperature) and subsequently tempered (annealed 1 h at 750°C) materials, long thermal ageing performed at temperatures between 250 and 550°C up to 22000 h, can induce an important Ductile-to-Brittle Transition Temperature (DBTT) shift directly related to the formation of new phases[3]. SANS measurements realised on several types of alloys (conventional and LAM) have shown different behaviours depending on the chemical composition. In particular, SANS was able to detect the formation of very small precipitates (nm size), not observed by TEM. For example, the formation of α' precipitates was observed by SANS in conventional and LAM alloys containing initial Cr content above 9% under thermal ageing at 400°C.
Some of these alloys were studied after fast neutron irradiation up to a dose of 0.8 d.p.a. (displacement per atom) at 325°C. In a Low Activation ("La4Ta") alloy containing 11.2%Cr, neutron irradiation induces an increase of the scattered intensity (figure 3) which can be attributed to the α-α' spinodal decomposition not observed under thermal ageing at this temperature. **In this case, the neutron irradiation induces accelerated phase separation**.
The "F82H" alloy presents no evolution under thermal ageing whatever the temperature as well as under irradiation up to 0.8 dpa. These behaviours are in qualitative agreement with the mechanical properties of the materials.

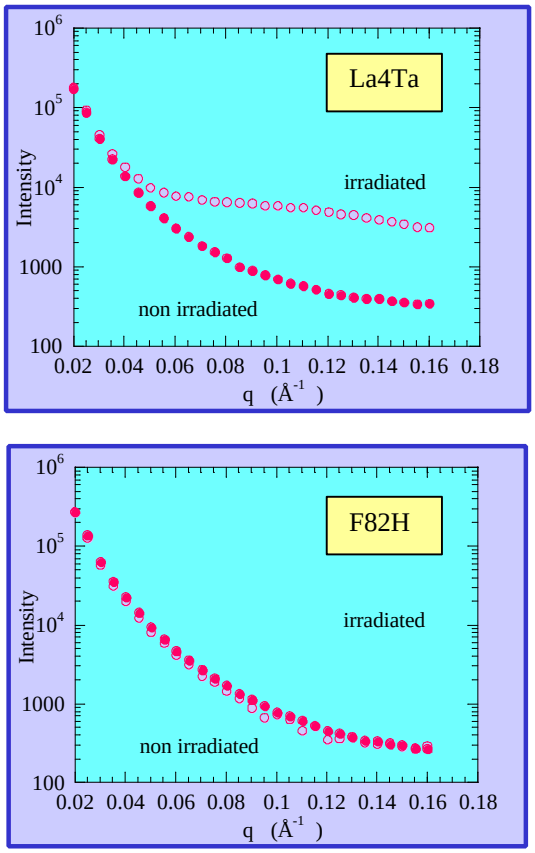

Figure 3 : SANS intensity scattered by two low activation alloys (F82H and La4Ta) before and after neutron irradiation.

In summary, the combined use of SANS and TEM allows to obtain a detailed description of precipitation. This study has put in evidence the role of the initial chemical composition on the alloys behaviour under thermal treatment or neutron irradiation. SANS measurements allowed a direct correlation of the microstructure evolution with the secondary hardening phenomenon.

1 Mathon M.H., Barbu A., Dunstetter F., Maury F., Lorenzelli N., de Novion C.H.., J. Nucl. Mat., **245** (1997) 224-237
2 Brachet J.C , J. Phys. III, C3, 4 (1994) 83
3 Brachet J.C., Castaing A., Foucher A., Note Technique SRMA 95-2140, august 1995